

# Numerical Solution of the Gross-Pitaevskii Equation

Shiyu Peng \*

November 25, 2018

## Abstract

This project report is for computational mathematics module. We use the Time-splitting spectral method to solve the time-dependent Gross–Pitaevskii equation (GPE) numerically. For comparison, we also use other two methods to solve this equation, one is Crank–Nicolson finite difference method, another is Crank–Nicolson spectral method. We conduct numerical experiments by using these three methods in 2-D GPE, and do the error estimation and control, also do the comparison among these three methods on the accuracy and the speed of computation. However, because of the computational limitations of the personal computer, we cannot reach an ideal accuracy which can only be achieved with a high-performance computer. We choose suitable parameters to test our code and get more accurate results as possible as we can.

**Keywords:** time-dependent Gross–Pitaevskii equation, Time-splitting spectral method, Crank–Nicolson finite difference method, Crank–Nicolson spectral method

---

\* Email: [pengshiyu23@yahoo.com](mailto:pengshiyu23@yahoo.com)

# 1. Introduction

This project report focuses on using the Time-splitting spectral method which is suitable for the time-dependent Gross–Pitaevskii equation (GPE). Also, we introduce Crank–Nicolson finite difference method and Crank–Nicolson spectral method. Our main contribution is an efficient MATLAB solver for the PDEs of this type. Since we focus on using these methods to solve the mathematical problems, we do not spend time explaining the physical meanings which are related to GPE.

The Time-splitting Fourier spectral method (TSSP) is the combination of the two techniques—time splitting discretisation and Fourier spectral methods which are both successfully applied to many PDE problems. This method is unconditionally stable, time reversible, time-transverse invariant, and conserves the total particle. It also has very favourable properties with respect to efficiently choosing the spatial/temporal grid in dependence of the semiclassical parameter  $\epsilon$ . And in this report, we also use two other method Crank-Nicolson finite difference scheme (CNFD) and Crank-Nicolson spectral method (CNSP) to solve the time-dependent Gross–Pitaevskii equation (GPE) for comparison. Both these two methods are unconditionally stable, time reversible, and conserves the total particle number but they are not time-transverse invariant.

The structure of remaining part of this report is as follow. In Section 2, we briefly describe the time-dependent Gross–Pitaevskii equation (GPE) and the way to simplify it. We then introduce three methods in Section 3. In Section 4, we introduce the approaches to do the error estimation and error control by [3][4], with an emphasize on error control. Section 5 includes our test results. We then make comparison and conclude.

## 2. Gross–Pitaevskii equation

Write time-dependent Gross–Pitaevskii equation as

$$i\hbar \frac{\partial \psi(r,t)}{\partial t} = \left(-\frac{\hbar^2}{2m} \nabla^2 + V(r) + g|\psi(r,t)|^2\right)\psi(r,t) \quad (2.1)$$

Here  $\hbar$  is the Planck constant,  $m$  is the atomic mass,  $\psi$  is the wave function. When we take a harmonic trap into consideration, the equation (2.1) becomes

$$i\hbar \frac{\partial \psi(X,t)}{\partial t} = -\frac{\hbar^2}{2m} \nabla^2 \psi(X,t) + \frac{m}{2} (\omega_x^2 x^2 + \omega_y^2 y^2 + \omega_z^2 z^2) \psi(X,t) + NU_0 |\psi(X,t)|^2 \psi(X,t) \quad (2.2)$$

Where  $X = (x, y, z)^T$  is the spatial coordinate vector,  $N$  is the number of atoms in the condensate, and  $\omega_x$ ,  $\omega_y$  and  $\omega_z$  are the trap frequencies in  $x$ -,  $y$ - and  $z$ -direction, respectively. We assume that  $\omega_x \ll \omega_y \ll \omega_z$  to simplify calculation. Besides  $U_0$  describes the interaction between atoms in the condensate and has the form

$$U_0 = \frac{4\pi\hbar^2 a}{m} \quad (2.3)$$

here  $a$  is the s-wave scattering length (positive for repulsive interaction and negative for attractive interaction). It is necessary to ensure that the wave function is properly normalized. Specifically, we require

$$\int_{R^3} |\psi(X,t)|^2 dx = 1 \quad (2.4)$$

### 2.1 Dimensionless GPE

After obtaining GPE as above, we choose to do dimensionless first, since it is helpful for us to solve GPE. We change some variable in order to scale Eq. (2.2) under normalization (2.4),

$$\tilde{t} = \omega_x t, \tilde{X} = \frac{X}{x_s}, \tilde{\psi}(\tilde{X}, \tilde{t}) = x_s^{3/2} \psi(X, t) \quad (2.5)$$

Then, plugging (2.5) into (2.2), multiplying by  $1/m\omega_x^2x_s^{1/2}$ , and removing all  $\sim$  terms, so we obtain the following dimensionless GPE in three spatial dimensions,

$$i\varepsilon \frac{\partial \psi(X,t)}{\partial t} = -\frac{\varepsilon^2}{2} \nabla^2 \psi(X,t) + V(X)\psi(X,t) + \delta \varepsilon^{5/2} |\psi(X,t)|^2 \psi(X,t) \quad (2.6)$$

Where

$$V(x) = \frac{1}{2}(x^2 + \gamma_y^2 y^2 + \gamma_z^2 z^2), \varepsilon = \frac{\hbar}{\omega_x m x_s^2} = \left(\frac{a_0}{x_s}\right)^2, \gamma_y = \frac{\omega_y}{\omega_x}, \gamma_z = \frac{\omega_z}{\omega_x},$$

$$\delta = \frac{U_0 N}{a_0^3 \hbar \omega_x} = \frac{4\pi a N}{a_0}, a_0 = \sqrt{\frac{\hbar}{\omega_x m}},$$

with  $a_0$  the length of the harmonic oscillator ground state (in  $x$ -direction). The coefficient of the nonlinearity of Eq. (2.6) can also be expressed as:

$$\kappa := \delta \varepsilon^{5/2} = \frac{\text{sgn}(a)}{2} \left( \frac{a_0}{x_h} \frac{a_0}{x_s} \right)^2 \quad (2.7)$$

here  $x_h$  is the healing length (see [1]) with

$$x_h := \left( \frac{8\pi |a| N}{x_s^3} \right)^{-1/2} \quad (2.8)$$

There are two extreme regimes: (i) when  $\varepsilon = O(1) (\Leftrightarrow a_0 = O(x_s))$  and  $\kappa = \delta \varepsilon^{5/2} = o(1) (\Leftrightarrow 4\pi |a| N \ll a_0)$ , then Eq. (2.6) describes a weakly interacting condensate. (ii) when  $\varepsilon = o(1) (\Leftrightarrow x_s \gg a_0)$  and  $\kappa = \delta \varepsilon^{5/2} = O(1)$  (implying  $4\pi |a| N \gg a_0$ ) (or  $\varepsilon = 1$  and  $\kappa = \delta \varepsilon^{5/2} = \delta$  with  $|\delta| \gg 1$  by the rescaling  $X \rightarrow \varepsilon^{1/2} X$ ,  $\psi \rightarrow \psi/\varepsilon^{3/4}$ ), then Eq. (2.6) describes a strongly interacting condensate.

We will discuss approximate ground state solution in two extreme regimes and then use solution to reduce the 3-D GPE to a 2-D GPE.

## 2.2 Approximate ground state solution in 3d

For general cases, we write

$$\psi(X, t) = \exp\left(-\frac{i\mu t}{\varepsilon}\right)\phi(X) \quad (2.9)$$

here  $\mu$  is the chemical potential of the condensate. We can get the following equation by inserting Eq. (2.9) into Eq. (2.6),

$$\mu\phi(X) = -\frac{\varepsilon^2}{2}\nabla^2\phi(X) + V(X)\phi(X) + \kappa|\phi(X)|^2\phi(X), \quad X \in \mathbb{R}^3. \quad (2.10)$$

under the normalization condition

$$\int_{\mathbb{R}^3} |\phi(X)|^2 dX = 1 \quad (2.11)$$

This is a nonlinear eigenvalue problem. Then we apply perturbation theory. Define the energy functional

$$E(\phi) := \frac{\varepsilon^2}{2} \int_{\mathbb{R}^3} |\nabla\phi|^2 dX + \int_{\mathbb{R}^3} V(x)|\phi|^2 dX + \frac{\kappa}{2} \int_{\mathbb{R}^3} |\phi|^4 dX \quad (2.12)$$

The Bose–Einstein condensate ground-state wave function  $\phi_g(X)$  is found by solving this eigenvalue problem under the normalization condition (2.11) with the minimal chemical potential  $\mu_g$ . It is easy to see that critical points of  $E$  are ‘eigenfunctions’ of the nonlinear Hamiltonian. Next, we solve the following equations to compute the ground state  $\phi_g$

$$E(\phi_g) = \min_{\int_{\mathbb{R}^3} |\phi|^2 dX = 1} E(\phi), \quad \mu_g = E(\phi_g) + \frac{\kappa}{2} \int_{\mathbb{R}^3} |\phi_g|^4 dX \quad (2.13)$$

For a weakly interacting condensate, we drop the nonlinear term and find the harmonic oscillator equation

$$\mu\phi(X) = -\frac{\varepsilon^2}{2}\nabla^2\phi(X) + \frac{1}{2}(x^2 + \gamma_y^2 y^2 + \gamma_z^2 z^2)\phi(X) \quad (2.14)$$

The ground state solution of (2.14) is

$$\mu_g^w = \frac{1+\gamma_y+\gamma_z}{2}\varepsilon, \quad \phi(X)_g^w = \frac{(\gamma_y\gamma_z)^{1/4}}{(\pi\varepsilon)^{3/4}} \exp\left(-(x^2 + \gamma_y^2 y^2 + \gamma_z^2 z^2)/2\varepsilon\right) \quad (2.15)$$

For a condensate with strong repulsive interactions, we drop the diffusion term corresponding to the Thomas–Fermi approximation:

$$\mu\phi(X) = V(X)\phi(X) + \kappa|\phi(X)|^2\phi(X), X \in \mathbb{R}^3 \quad (2.16)$$

The ground state solution is that

$$\mu_g^s = \frac{\varepsilon}{2} \left( \frac{15\delta\gamma_y\gamma_z}{4\pi} \right)^{\frac{2}{5}} = \frac{1}{2} \left( \frac{15\kappa\gamma_y\gamma_z}{4\pi} \right)^{\frac{2}{5}}, \phi_g^s(X) = \begin{cases} \sqrt{(\mu_g^s - V(X))/\kappa}, & V(X) < \mu_g^s \\ 0, & \text{otherwise.} \end{cases} \quad (2.17)$$

These approximate ground state solutions are used in reducing the 3-D GPE to a 2-D GPE and a 1-D GPE and as initial data for the numerical solution of the time-dependent GPE in Section 4.

## 2.3 Reduction to lower dimensions

In two important cases, the 3-D Gross–Pitaevskii Eq. (2.6) can approximately be reduced to a lower dimensional PDE. We only discuss the way how to reduce the 3-D GPE to 2-D GPE, since we use it in our Numerical experiments. Firstly, consider the total condensate energy

$$E[\psi(t)] = \frac{\varepsilon^2}{2} \int_{\mathbb{R}^3} |\nabla\psi(t)|^2 dX + \frac{1}{2} \int_{\mathbb{R}^3} (x^2 + \gamma_y^2 y^2) |\psi(t)|^2 dX + \frac{\gamma_z^2}{2} \int_{\mathbb{R}^3} z^2 |\psi(t)|^2 dX + \frac{\kappa}{2} \int_{\mathbb{R}^3} |\psi(t)|^4 dX \quad (2.18)$$

Multiplying (2.6) by  $\overline{\psi_t}$  and integrating by parts show the energy conservation

$$E[\psi(t)] = E[\psi_I] \quad \forall t \quad (2.19)$$

where  $\psi_I = \psi(t = 0)$  is the initial function which may depend on all parameters  $\varepsilon, \gamma_y, \gamma_z$  and  $\kappa$ . Now assume that  $\psi_I$  satisfies

$$\frac{E[\psi_I]}{\gamma_z^2} \rightarrow 0 \quad \text{as } \gamma_z \rightarrow \infty \quad (2.20)$$

Then the 3d GPE (2.6), and 2d GPE can then be written in a unified way

$$i\varepsilon \frac{\partial\psi(X,t)}{\partial t} = -\frac{\varepsilon^2}{2} \nabla^2 \psi(X,t) + V_d(X)\psi(X,t) + \kappa_d |\psi(X,t)|^2 \psi(X,t), X \in \mathbb{R}^d \quad (2.21)$$

where

$$\kappa_d = \delta \varepsilon^{5/2} \begin{cases} \int_{\mathbb{R}} \psi_3^4(z) dz, \\ 1, \end{cases}, \quad V_d(X) = \begin{cases} \frac{1}{2}(x^2 + \gamma_y^2 y^2), & d = 2, \\ \frac{1}{2}(x^2 + \gamma_y^2 y^2 + \gamma_z^2 z^2), & d = 3, \end{cases} \quad (2.22)$$

The normalization condition for (2.21) is

$$\int_{\mathbb{R}^4} |\psi(X, t)|^2 dX = 1 \quad (2.23)$$

By using the approximate ground state of Section 2.2, we derive – after simple calculations – for a weakly interacting condensate

$$\kappa_d := \kappa_d^w = \begin{cases} \kappa \sqrt{\frac{\gamma_z}{2\pi\varepsilon}} = \delta \varepsilon^{4/2} \sqrt{\frac{\gamma_z}{2\pi}}, & d = 2, \\ \kappa = \delta \varepsilon^{5/2}, & d = 3, \end{cases} \quad (2.24)$$

and for a condensate with strong repulsive interactions

$$\kappa_d := \kappa_d^s = \begin{cases} \left( \frac{5}{7} \left( \frac{4\pi}{15} \right)^{1/5} \frac{(\kappa \gamma_z)^{4/5}}{\gamma_y^{1/5}} = (\delta \gamma_z)^{4/5} \varepsilon^{4/2} \left( \frac{4\pi}{15\gamma_y} \right)^{1/5} \frac{5}{7}, & d = 2 \\ \kappa = \delta \varepsilon^{5/2}, & d = 3. \end{cases} \quad (2.25)$$

### 3. Numerical methods used in experiments

In this section, we use three methods to solve 2-D GPE. They are Time-splitting spectral method (TSSP), Crank–Nicolson finite difference method (CNFD) and Crank–Nicolson spectral method (CNSP). Firstly, we use TSSP method, the merit of this method is that it is unconditionally stable, time reversible, time-transverse invariant, and conserves the total particle number. Also, it has very favourable properties with respect to efficiently choosing the spatial / temporal grid in dependence of the semiclassical parameter  $\varepsilon$ . Now we derive the 2-D case of these methods in example 3. For  $d = 2$ , Eq. (2.21) with periodic boundary conditions becomes

$$i\varepsilon \frac{\partial \psi(x,t)}{\partial t} = -\frac{\varepsilon^2}{2} (\psi_{xx}(x,t) + \psi_{yy}(x,y)) + \frac{x^2 + y^2}{2} \psi(x,t) + \kappa_2 |\psi(x,t)|^2 \psi(x,t).$$

$$\psi(x, y, t = 0), \quad a \leq x, y \leq b.$$

$$\psi(a, y, t) = \psi(b, y, t), \psi(x, a, t) = \psi(x, b, t).$$

$$\psi_x(a, y, t) = \psi_x(b, y, t), \psi_y(x, a, t) = \psi_y(x, b, t).$$

#### 3.1 Time-splitting spectral method (TSSP) (Explicit Scheme):

Initial phrase:

$$\psi(x, y, 0) = \frac{1}{\sqrt{\pi\varepsilon}} \exp\left(-\frac{x^2 + y^2}{2\varepsilon}\right)$$

Boundary condition (periodic):

$$\psi(-10, y, t) = \psi(10, y, t), \psi(x, -10, t) = \psi(x, 10, t),$$

$$\psi_x(-10, y, t) = \psi_x(10, y, t), \psi_y(x, -10, t) = \psi_y(x, 10, t)$$

Spatial mesh size and Time step:



$$h = \frac{20}{N}, x_q = -10 + qh, y_j = -10 + jh, t_n = nk$$

From  $t_n \rightarrow t_{n+1}$ :

We write

$$i\varepsilon\psi_t = -\frac{\varepsilon^2}{2}(\psi_{xx} + \psi_{yy}) \quad (3.1)$$

Then discretizing it in space by Fourier spectral method and integrated in time, leaving  $|\psi(x, t)|^2$  invariant:

$$i\varepsilon \frac{\partial \psi(x, t)}{\partial t} = \frac{x^2 + \gamma_y y^2}{2} \psi(x, t) + \kappa_2 |\psi(x, t_n)|^2 \psi(x, t)$$

Then solving the following ODE:

$$\psi_{q,j}^* = \exp\left(\frac{-i\left(\frac{x_q^2 + \gamma_y^2 y_j^2}{2} + \kappa_2 |\psi_{q,j}^n|^2\right)\kappa}{2\varepsilon}\right) \psi_{q,j}^n$$

The Fourier coefficient of  $\psi^*$ :

$$\hat{\psi}_{l_1, l_2}^* = \sum_{q=0}^{N-1} \sum_{j=0}^{N-1} \psi_{q,j}^* \exp\left(-i\mu_{l_1}(x_q + 10) - i\mu_{l_2}(y_j + 10)\right) \quad (3.2)$$

Where  $\mu_{l_1} = \frac{2\pi l_1}{20}, \mu_{l_2} = \frac{2\pi l_2}{20}, l_1, l_2 = -\frac{N}{2}, \dots, \frac{N}{2} - 1$ .

We use the result of (3.2) and apply it to (3.1):

$$\psi_{q,j}^{**} = \frac{1}{N^2} \sum_{l_1=-N/2}^{N/2-1} \sum_{l_2=-N/2}^{N/2-1} \exp\left(\frac{-i\varepsilon\kappa(\mu_{l_1}^2 + \mu_{l_2}^2)}{2}\right) \hat{\psi}_{l_1, l_2}^* \exp\left(i\mu_{l_1}(x_q + 10) + i\mu_{l_2}(y_j + 10)\right) \quad (3.3)$$

Substituting (3.3) to the solution of the ODE and getting:

$$\psi_{q,j}^{n+1} = \exp\left(\frac{-i\left(\frac{x_q^2 + \gamma_y^2 y_j^2}{2} + \kappa_2 |\psi_{q,j}^{**}|^2\right)\kappa}{2\varepsilon}\right) \psi_{q,j}^{**}$$

Then we can use this explicit scheme to solve the 2-D Gross–Pitaevskii equation numerically.

### 3.2 Crank–Nicolson finite difference (CNFD) (Implicit Scheme):

$$i\varepsilon \frac{\partial \psi(x, t)}{\partial t} = -\frac{\varepsilon^2}{2}(\psi_{xx} + \psi_{yy}) + \frac{x^2 + \gamma_y^2 y^2}{2} \psi(x, t) + \kappa_2 |\psi(x, t)|^2 \psi(x, t)$$

Discretize the equation at point  $(x_q, y_j, t_{n+\frac{1}{2}})$ :

$$\begin{aligned} \psi_t &= \frac{\psi_{q,j}^{n+1} - \psi_{q,j}^n}{\kappa} \\ \psi_{xx} &= \frac{1}{2} \left( \frac{\psi_{q+1,j}^{n+1} - 2\psi_{q,j}^{n+1} + \psi_{q-1,j}^{n+1}}{h^2} + \frac{\psi_{q+1,j}^n - 2\psi_{q,j}^n + \psi_{q-1,j}^n}{h^2} \right) \\ \psi_{yy} &= \frac{1}{2} \left( \frac{\psi_{q,j+1}^{n+1} - 2\psi_{q,j}^{n+1} + \psi_{q,j-1}^{n+1}}{h^2} + \frac{\psi_{q,j+1}^n - 2\psi_{q,j}^n + \psi_{q,j-1}^n}{h^2} \right) \\ \psi &= \frac{1}{2}(\psi_{q,j}^{n+1} + \psi_{q,j}^n) \end{aligned}$$

Also leave the term  $|\psi(x, t)|^2$  invariant and substitute  $\psi_x$ ,  $\psi_{xx}$ ,  $\psi_{yy}$ ,  $\psi$  to the equation, truncate and rearrange:

$$\begin{aligned} \left( \frac{i\varepsilon}{\kappa} - \frac{\varepsilon^2}{h^2} - \frac{\frac{x_q^2 + \gamma_y^2 y_j^2}{2} + \kappa_2 |\psi_{q,j}^n|^2}{2} \right) \psi_{q,j}^{n+1} + \frac{\varepsilon^2}{4h^2} \psi_{q+1,j}^{n+1} + \frac{\varepsilon^2}{4h^2} \psi_{q-1,j}^{n+1} + \frac{\varepsilon^2}{4h^2} \psi_{q,j+1}^{n+1} + \frac{\varepsilon^2}{4h^2} \psi_{q,j-1}^{n+1} = \\ \left( \frac{i\varepsilon}{\kappa} + \frac{\varepsilon^2}{h^2} + \frac{\frac{x_q^2 + \gamma_y^2 y_j^2}{2} + \kappa_2 |\psi_{q,j}^n|^2}{2} \right) \psi_{q,j}^n - \frac{\varepsilon^2}{4h^2} \psi_{q+1,j}^n - \frac{\varepsilon^2}{4h^2} \psi_{q-1,j}^n - \frac{\varepsilon^2}{4h^2} \psi_{q,j+1}^n - \frac{\varepsilon^2}{4h^2} \psi_{q,j-1}^n \end{aligned}$$

$$n = 0, 1, \dots, N_t - 1, \quad q, j = 1, \dots, N$$

Boundary condition (Periodic):

$$\psi_{0,j}^n = \psi_{N,j}^n, \psi_{q,0}^n = \psi_{q,N}^n, \psi_{1,j}^n = \psi_{N+1,j}^n, \psi_{q,1}^n = \psi_{q,N+1}^n, \psi_{q,j}^0 = \psi(x_q, y_j, 0)$$

Then solve the linear system.

### 3.3 Crank–Nicolson spectral method (CNSP) (Implicit Scheme):

We write Crank-Nicolson local discretization and leave  $|\psi(x, t)|^2$  invariant:

$$i\varepsilon \frac{\psi_{q,j}^{n+1} - \psi_{q,j}^n}{k} = -\frac{\varepsilon^2}{2}(\psi_{xx} + \psi_{yy}) + \frac{\psi_{q,j}^{n+1} + \psi_{q,j}^n}{2} \left( \frac{x_q^2 + y_j^2}{2} + \kappa_2 |\psi_{q,j}^n|^2 \right) \quad (3.4)$$

Then we use spectral differential operator  $\delta_{xx}$  and  $\delta_{yy}$  to approximate  $D_{xx}^f$  and  $D_{yy}^f$  respectively:

$$D_{xx}^f \psi^{n+1}|_{x=x_q, y=y_j} = - \sum_{l_1=-N/2}^{N/2-1} \sum_{l_2=-N/2}^{N/2-1} \mu_{l_1}^2 (\hat{\psi}^{n+1})_{l_1, l_2} \exp(i\mu_{l_1}(x_q + 10) + i\mu_{l_2}(y_j + 10))$$

Where  $(\hat{\psi}^{n+1})_{l_1, l_2} = \sum_{q=0}^{N-1} \sum_{j=0}^{N-1} \psi_{q,j}^{n+1} \exp(-i\mu_{l_1}(x_q + 10) - i\mu_{l_2}(y_j + 10))$

$$\mu_{l_1} = \frac{2\pi l_1}{20}, \mu_{l_2} = \frac{2\pi l_2}{20}$$

It is very similar to define  $D_{xx}^f \psi^n, D_{xx}^f \psi^{n+1}, D_{yy}^f \psi^{n+1}, D_{yy}^f \psi^n$ ,

$$\text{Let } \psi_{xx} \approx \frac{1}{2}(D_{xx}^f \psi^{n+1} + D_{xx}^f \psi^n), \psi_{yy} \approx \frac{1}{2}(D_{yy}^f \psi^{n+1} + D_{yy}^f \psi^n)$$

Then substitute them to (3.4), we get a linear system and solve it.

## 4. Error estimation and Error control

In [3][4], the authors give a uniform error bound for both first and second order method, with and without damping. We only mention those results.

The TSSP method is unconditionally stable, time reversible, time-transverse invariant, and conserves the total particle.

Both CNFD and CNSP methods are also unconditionally stable, time reversible, conserve the total particle number but they are not time transverse-invariant.

According to the paper and some other papers [3][4], for the TSSP method, the overall time discretization error is  $O(k^2)$  for fixed  $\varepsilon > 0$ , which means temporal discretization errors are of second order accuracy. The spatial errors are of spectral order accuracy. The admissible meshing strategy is  $k = O(\varepsilon)$  and  $h = O(\varepsilon)$ .

For CNFD method, the spatial and temporal discretization errors are of second and first order respectively, the admissible meshing strategy is  $k = o(\varepsilon)$  and  $h = o(\varepsilon)$  which is more restrictive compared to TSSP.

For CNSP method, the spatial and temporal discretization errors are of spectral and first order accuracy respectively. The admissible meshing strategy is  $k = o(\varepsilon)$  and  $h = O(\varepsilon)$

	TSSP	CNFD	CNSP
Spatial	Spatial order	Second order	Spatial order
Temporal	Second order	First order	First order

There is a specific requirement for weak case and strong case. As the paper describing, when the case is weakly interacting condensate,  $\varepsilon$  is equal to  $O(1)$ , and when the case is strong interacting condensate,  $\varepsilon$  is  $\ll 1$  and is described as  $o(1)$ . The  $\varepsilon$  in the strong case is much smaller than it in the weak case. That means in order to obtain the ‘correct’ observation, we need the meshing strategy to be more restrictive in the strong case than the weak case.

Now we cite the proof and theorem for error analysis from [3]:

Let  $u = (U_0, \dots, U_{M-1})^T$ . Let  $\|\cdot\|_{L^2}$  and  $\|\cdot\|_{l^2}$  be the usual  $L^2$ -norm and discrete  $l^2$ -norm respectively on the domain.

$$\|u\|_{L^2} = \sqrt{\int_a^b |u(x)|^2 dx}, \quad \|\mathbf{u}\|_{l^2} = \sqrt{\frac{b-a}{M} \sum_{j=0}^{M-1} |U_j|^2}.$$

**Lemma 3.1.[3]** TSSP is unconditionally stable. In fact, under any mesh size  $h$  and time steps,

$$\|\mathbf{u}^{\varepsilon, n}\|_{l^2} = \|u_0^\varepsilon\|_{l^2}, \quad n = 1, 2, \dots,$$

**Proof.**

Noted that the identities:

$$\sum_{j=0}^{M-1} e^{i2\pi(k-l)j/M} = \begin{cases} 0, & k-l \neq mM, \\ M, & k-l = mM, \end{cases} \quad m \text{ integer}$$

$$\sum_{l=-M/2}^{\frac{M}{2}-1} e^{i2\pi(k-j)l/M} = \begin{cases} 0, & k-j \neq mM, \\ M, & k-j = mM, \end{cases} \quad m \text{ integer}.$$

The Fourier coefficients of  $\mathbf{U}^{\varepsilon, *}$ :

$$\hat{U}_l^{\varepsilon, *} = \sum_{j=0}^{M-1} U_j^{\varepsilon, *} e^{-i\mu_l(x_j-a)}, \quad l = -\frac{M}{2}, \dots, \frac{M}{2} - 1.$$

For the TSSP method:

$$\begin{aligned} \frac{1}{b-a} \|\mathbf{u}^{\varepsilon, n+1}\|_{l^2}^2 &= \frac{1}{M} \sum_{j=0}^{M-1} |U_j^{\varepsilon, n+1}|^2 = \frac{1}{M} \sum_{j=0}^{M-1} \left| e^{-\frac{iV(x_j)k}{2\varepsilon}} U_j^{\varepsilon, **} \right|^2 = \frac{1}{M} \sum_{j=0}^{M-1} |U_j^{\varepsilon, **}|^2 = \\ \frac{1}{M} \sum_{j=0}^{M-1} \left| \frac{1}{M} \sum_{l=-\frac{M}{2}}^{\frac{M}{2}-1} e^{-\frac{i\varepsilon k u_l^2}{2}} \hat{U}_l^{\varepsilon, *} e^{i\mu_l(x_j-a)} \right|^2 &= \frac{1}{M^2} \sum_{l=-\frac{M}{2}}^{\frac{M}{2}-1} \left| e^{\frac{i\varepsilon k \mu_l^2}{2}} \hat{U}_l^{\varepsilon, *} \right|^2 = \frac{1}{M^2} \sum_{l=-\frac{M}{2}}^{\frac{M}{2}-1} |\hat{U}_l^{\varepsilon, *}|^2 = \\ \frac{1}{M^2} \sum_{l=-\frac{M}{2}}^{\frac{M}{2}-1} \left| \sum_{j=0}^{M-1} U_j^{\varepsilon, *} e^{-i\mu_l(x_j-a)} \right|^2 &= \frac{1}{M} \sum_{j=0}^{M-1} |U_j^{\varepsilon, *}|^2 = \frac{1}{M} \sum_{j=0}^{M-1} \left| e^{-\frac{iV(x_j)k}{2\varepsilon}} U_j^{\varepsilon, n} \right|^2 = \\ \frac{1}{M} \sum_{j=0}^{M-1} |U_j^{\varepsilon, n}|^2 &= \frac{1}{b-a} \|\mathbf{u}^{\varepsilon, n}\|_{l^2}^2. \end{aligned}$$

The proof of error estimates for TSSP involves more complicated calculations and will be omitted here.

**Theorem 5.1.[3]**

For CNFD method:

$$l_{CNFD}^{\varepsilon,n} = O(k^2 \|u_{ttt}^\varepsilon\|_{L_t^\infty(L_x^2)}) + O(h^2 \varepsilon \|u_{xxxx}^\varepsilon\|_{L_t^\infty}) = O\left(C_3 \frac{k^2}{\varepsilon^3} + C_4 \frac{h^2}{\varepsilon^3}\right).$$

The global  $L^2$ -error of CNFD is

$$\|u^\varepsilon(t_n) - u^{\varepsilon,n}\|_{L^2} = O\left(\left(C_3 \frac{k^2}{\varepsilon^3} + C_4 \frac{h^2}{\varepsilon^3}\right) T\right).$$

**Theorem 5.2.[3]**

For CNSP method:

$$l_{CNSP}^{\varepsilon,n} = O\left(k^2 \|u_{ttt}^\varepsilon\|_{L_t^\infty(L_x^2)}\right) + O\left(C_m \left(\frac{h}{(b-a)\varepsilon}\right)^{m-2} \frac{1}{\varepsilon}\right).$$

The global error of CNSP is

$$\|u^\varepsilon(t_n) - u_l^{\varepsilon,n}\|_{L^2} = O\left(\left(C_3 \frac{k^2}{\varepsilon^3} + C_m \left(\frac{h}{(b-a)\varepsilon}\right)^{m-2} \frac{1}{\varepsilon}\right) T\right).$$

## 5. Numerical experiments results

Due to the equipment constraints, we cannot reach the ideal accuracy. In order to match the meshing strategy for weak case where  $k = O(\varepsilon)$  and  $h = O(\varepsilon)$  in TSSP method, we use  $h = 0.1$ ,  $k = 0.0025$ ,  $T = 0.075$  (in the example,  $\varepsilon = 1$ ) to simulate the example 3 in [1] and test our codes.

For the (I)  $O(1)$ -interactions case, we get the TSSP results:

**Fig 1.** TSSP method,  
 $T = 0.075$

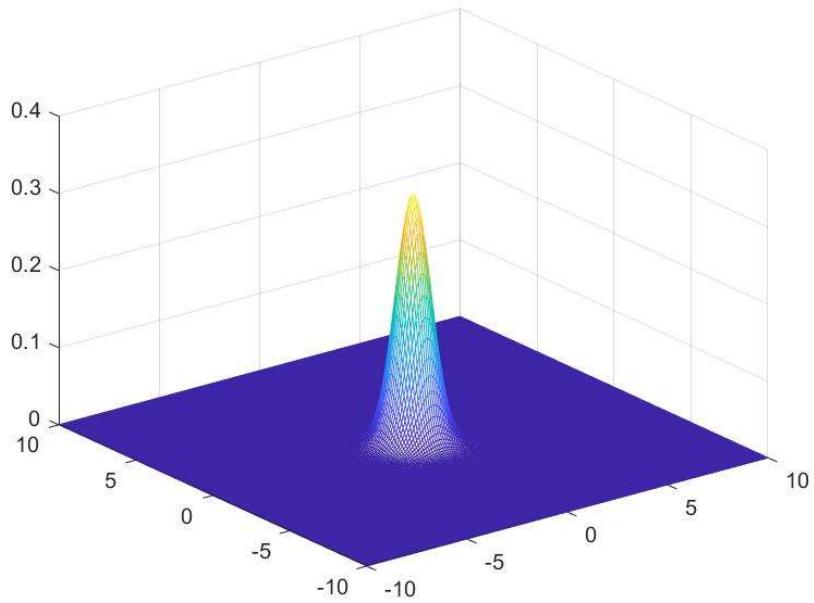
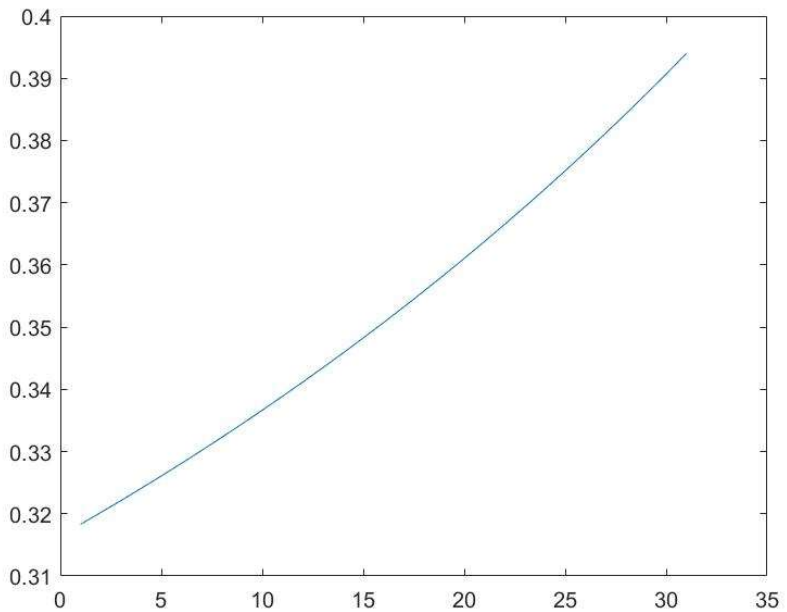


**Fig 2.** TSSP method,  
value of the position  
density  $|\psi(0,0,t)|^2$   
as a function of time,  
up to  $T = 0.075$



To test the method CNFD, we also use  $h = 0.4$ ,  $k = 0.0025$ ,  $T = 0.075$ . But the parameter is not small enough, in order to get ‘good’ observation, the parameters should be  $k = o(\varepsilon)$  and  $h = o(\varepsilon)$ , and in this case  $= 1$ . The number of operations per time step for CNFD is  $O(M)$ , that means if we reduce the  $h$  to its  $\frac{1}{10}$ , the number of operations per time step will be 100 times its previous number in 2-D case, the time used to run code will be about 100 times as using previous parameters, it takes too much time to run code with these small parameters.

**Fig 3.** CNFD method,  
 $T = 0.075$

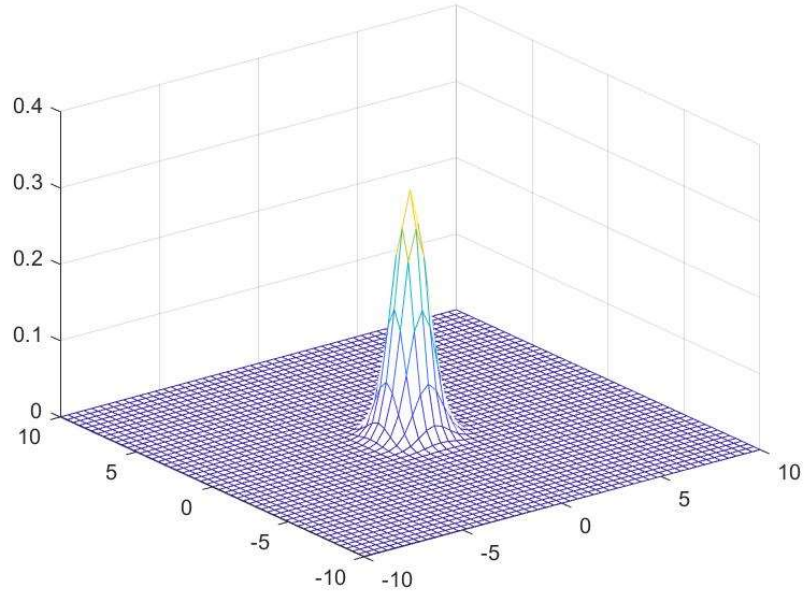
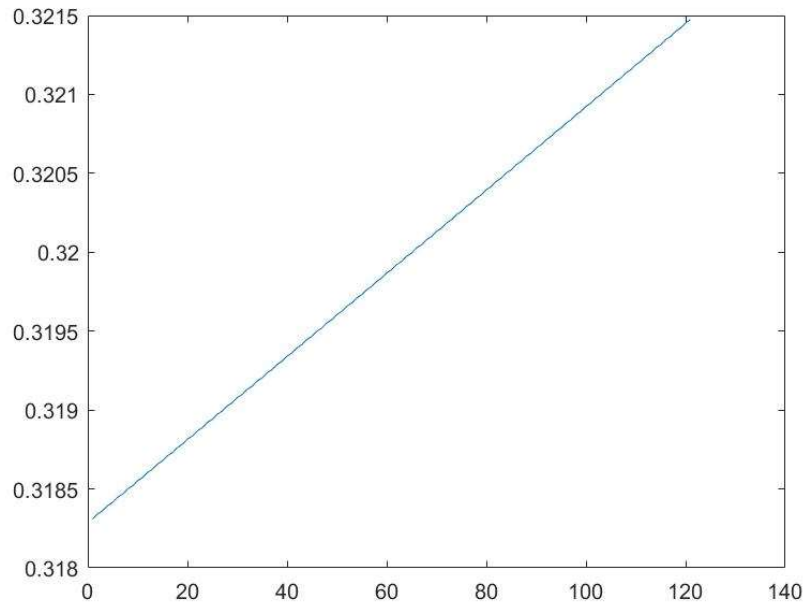


**Fig 4.** CNFD method,  
value of the position  
density  $|\psi(0,0,t)|^2$   
as a function of time,  
up to  $T = 0.3$





To test the method CNSP, we also use  $h = 1$ ,  $k = 0.00005$ ,  $T = 0.00025$ . In to get ‘correct’ observation, the requirement should be  $k = o(\varepsilon)$  and  $h = O(\varepsilon)$ . And in this method, the number of operations per time step is  $O(M^2)$ , if we reduce the parameter to its  $\frac{1}{10}$ , the number of operations per time step increases to its  $10^4$  times in 2-D case, the time to run code will increases to its  $10^4$  times. So, we need to choose parameter to be small enough to match  $k = o(\varepsilon)$  and  $h = O(\varepsilon)$ , and big enough for practical consideration.

**Fig 5.** CNSP method,  
 $T = 0.00025$

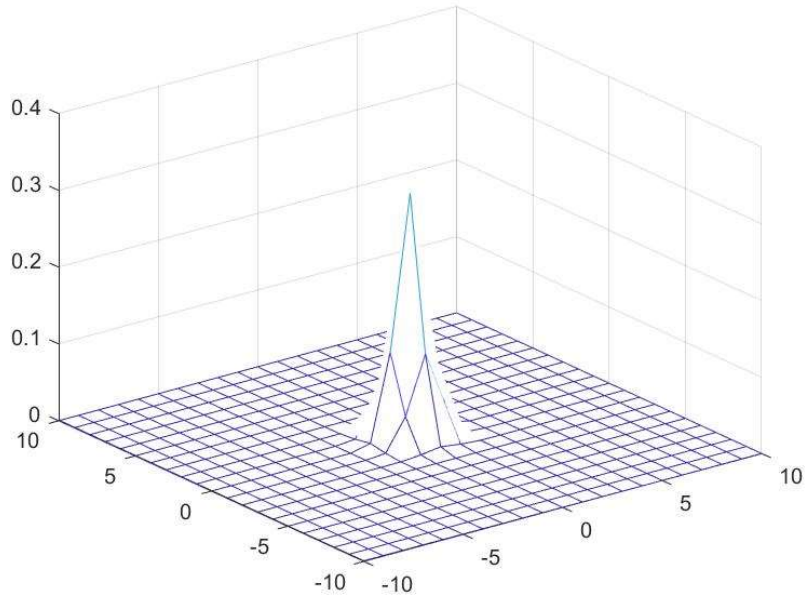
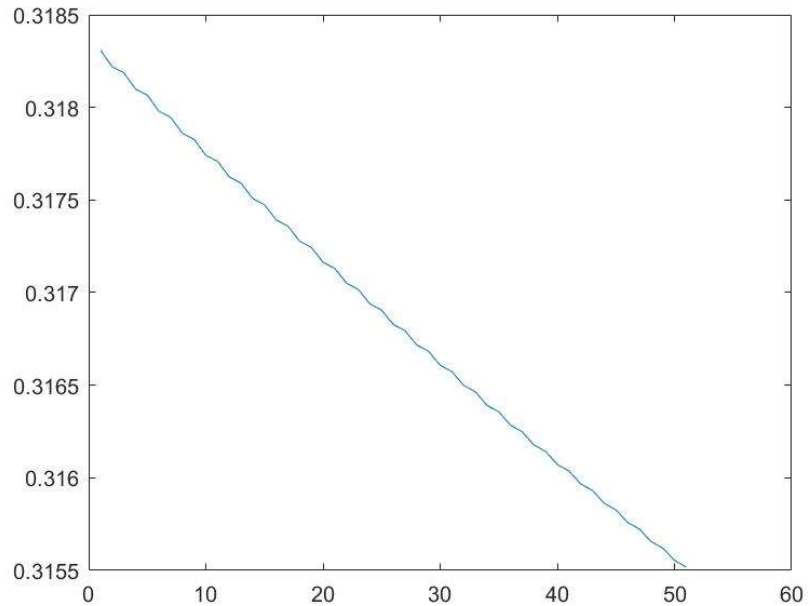
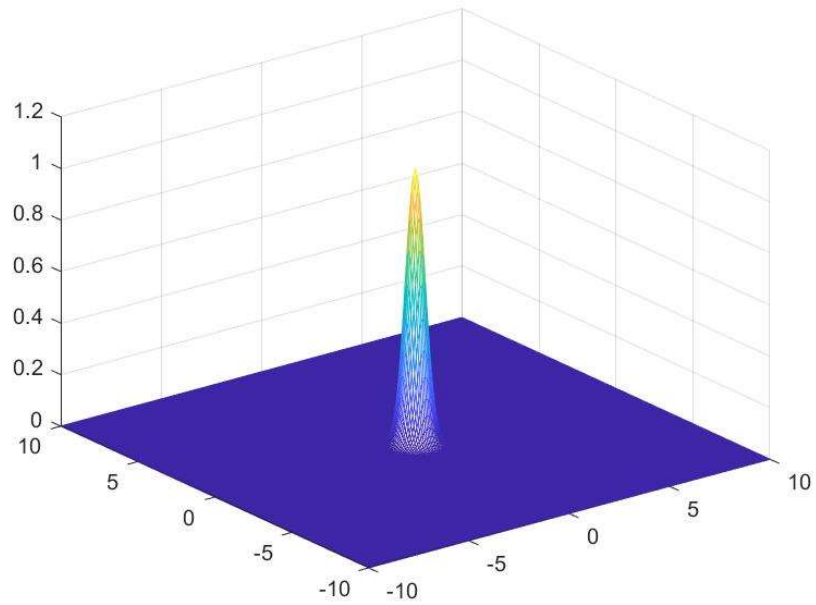


**Fig 6.** CNSP method,  
value of the position  
density  $|\psi(0,0,t)|^2$   
as a function of time,  
up to  $T = 0.0025$



For the (II) strong case, the  $\varepsilon$  is 0.3, the requirement to get the ‘correct’ observation is too constrained. Using laptop is hard to do that. For this case, we only simulate the TSSP method which has smaller computation requirement with the parameters  $h = 0.08$ ,  $k = 0.00005$  and  $T = 0.0001$ , the rest two methods used in strong case we attach their MATLAB codes for the simulation.

**Fig 7.** TSSP method  
(Strong),  $T =$   
0.0001



## 6. Conclusions

In this project report, we use the Time-splitting spectral method, Crank–Nicolson finite difference method and Crank–Nicolson spectral method to solve the 2-D time-dependent Gross–Pitaevskii equation (GPE) numerically.

For the comparison on accuracy, with the same computational cost, we find that Time-splitting spectral method is the best method among these three methods, then the second best one is Crank–Nicolson finite difference method, the last one is Crank–Nicolson spectral method.

For the comparison on the speed of computation, with the same accuracy, the result is also Time-splitting spectral method is the best method, then the second best one is Crank–Nicolson finite difference method, the last one is Crank–Nicolson spectral method.

# References

- [1]: Weizhu Bao, Dieter Jaksch and Peter A. Markowich. Numerical Solution of the Gross-Pitaevskii Equation for Bose-Einstein Condensation. *Journal of Computational Physics* 187 (2003) 318–342.
- [2]: S.K. Adhikari, Numerical study of the spherically symmetric Gross–Pitaevskii equation in two space dimensions, *Phys. Rev. E* 62 (2) (2000) 2937–2944.
- [3]: W. Bao, S. Jin, P.A. Markowich, On time-splitting spectral approximations for the Schrödinger equation in the semiclassical regime, *J. Comput. Phys.* 175 (2002) 487–524.
- [4]: W. Bao, S. Jin, P.A. Markowich, Numerical study of time-splitting spectral discretizations of nonlinear Schrödinger equations in the semi-classical regimes, *SIAM J. Sci. Comput.*, to appear.
- [5]: M.M. Cerimele, M.L. Chiofalo, F. Pistella, S. Succi, M.P. Tosi, Numerical solution of the Gross–Pitaevskii equation using an explicit finite-difference scheme: an application to trapped Bose–Einstein condensates, *Phys. Rev. E* 62 (1) (2000) 1382–1389.